

## Performance of Au transmission photocathode on a microchannel plate detector<sup>a)</sup>

M. E. Lowenstern, E. C. Harding, C. M. Huntington, A. J. Visco,  
G. Rathore, and R. P. Drake

*University of Michigan, 2455 Hayward Street, Ann Arbor, Michigan 48109, USA*

(Presented 13 May 2008; received 12 May 2008; accepted 23 July 2008;  
published online 31 October 2008)

X-ray framing cameras, employing microchannel plates (MCPs) for detection and signal amplification, play a key role in research in high-energy-density physics. These instruments convert radiographic x-rays into electrons produced by plasma during such experiments into electrons that are amplified in the channels and then detected by a phosphor material. The separation of detection from signal amplification offers potential improvements in sensitivity and noise properties. We have implemented a suspended Au transmission photocathode (160 Å thick) on a MCP and are evaluating it using a 1.5 keV Al  $K\alpha$  x-ray source. We find an approximately twofold increase in the ratio of detected events to incident photons when the photocathode-to-MCP voltage difference is sufficiently large. Our calculations indicate that this increase is probably caused by a combination of signal produced by the photocathode and an increase in the efficiency of detection of x-rays that reach the MCP surface through modification of the local electric field. © 2008 American Institute of Physics. [DOI: 10.1063/1.2971970]

### I. INTRODUCTION

The x-ray framing camera is an important radiographic tool employed in the field of inertial confinement fusion and high-energy-density physics to diagnose a wide variety of phenomena, including the evolution of hydrodynamic instabilities for which time resolved imaging is necessary. In present-day instrumentation these framing cameras typically use a microchannel plate (MCP) for detection, signal amplification, and gating.<sup>1</sup> The gating is accomplished by incorporating the MCP as a transmission line in an electronic pulse-forming circuit.<sup>2,3</sup> The amplification results from electron multiplication as initial photoelectrons and later secondary electrons are accelerated down the pores in the MCP, producing additional secondary electrons upon impact with the walls of the pore.<sup>4</sup> Our concern here is with detection. In many experiments the number of photons available for imaging is limited, making the quantum efficiency (QE) of the detector extremely important. Thus, much work has been done to examine the QE of MCPs. Specifically, the present work reports measurements using a suspended transmission photocathode (TPC) as a detecting element.

It has been suggested<sup>5</sup> that the use of a TPC suspended above a MCP may increase the detection efficiency of the photocathode/MCP system when detecting x-rays around 1 keV. One previous experimental effort reported by Ze *et al.*,<sup>6</sup> addressed this possibility. They observed an increase in signal when using a CsI coated photocathode placed in direct contact with a MCP. However, they did not compare this to a CsI coated MCP with no photocathode. In the present work,

we report the implementation of a suspended Au TPC above a nichrome-coated MCP, and measurements of the overall QE.

### II. THEORY

If a TPC is suspended some distance above the input face of the MCP, the incoming photons will first strike the TPC. Some of these photons will be absorbed in the TPC, which may lead to the emission of one or more secondary electrons from the rear surface. Such secondary electrons are then accelerated toward the MCP. The advantage of using a TPC lies in the fact that the energy of the electrons incident on the MCP can be adjusted by varying the potential difference between the TPC and the MCP so that the electron energy is equal to electron energy at which the MCP has its highest QE for electrons. For typical leaded MCP glass with incident electrons striking at 13°, Fraser<sup>7</sup> reported that this maximum electron QE occurs around electron energies of 500 eV, and is essentially unity.

Complications are introduced by the fact that the walls of the MCP pores have finite thickness so that the fraction of the MCP surface occupied by the pores (known as the “open area fraction”) is typically ~64%. The interpore area and the ends of the pores are coated with a conductor, typically to a depth of about one pore diameter. We will refer to this region as the “pore ends.” The pore ends are often overcoated with a photocathode material, but not in the present case, which would typically be described as a “bare” MCP, although in fact the pore ends are nichrome coated so that a voltage can be applied. The resulting connected surface establishes the electric potential near the entrance to the pores but gives it a complex structure. In some regions, the fields attract the

<sup>a)</sup> Contributed paper, published as part of the Proceedings of the 17th Topical Conference on High-Temperature Plasma Diagnostics, Albuquerque, New Mexico, May 2008.

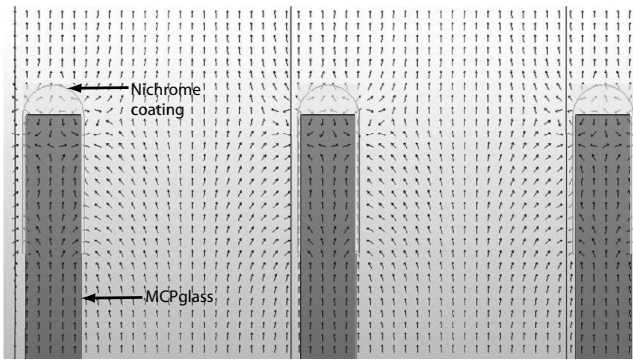


FIG. 1. Electric field structure. The arrows show the direction of the electric field from a two-dimensional model corresponding to a series of parallel channels of the same dimensions as the pores in the MCP, with a voltage that is 300 V lower established at a plane 210  $\mu\text{m}$  above the channel tops. Channel diameter is 10  $\mu\text{m}$  and channel walls are 2  $\mu\text{m}$  thick.

electrons to the conducting surfaces, tending to inhibit their amplification. With or without a TPC, it remains unclear to what extent secondary electrons produced on the MCP surface or very near the ends of the pores are detected.

To gain some insight into these effects we used the commercially available code LORENTZ-2E to model the electric fields in a system similar to the one used in our experiments. Figure 1 shows the results. The calculation, in two dimensions, modeled the pores as dielectric walls, 2  $\mu\text{m}$  thick, spaced 12  $\mu\text{m}$ , perpendicular to the TPC, and coated near their ends by a conductor, and modeled the TPC as a constant-voltage plane 210  $\mu\text{m}$  above the MCP surface. The figure is for a voltage difference of 300 V between the TPC and the MCP. One can see that the conducting pore ends affect the field, and will cause some electrons to strike the conducting surfaces. At smaller voltage differences, the electric field is more distorted by the pore ends, a larger fraction of the incident electrons is pulled onto the conducting surfaces, and a smaller fraction of the conducting surface readily releases electrons down into the pore. As a result, any increase in signal observed with a TPC might include contributions from changes to the detection efficiency of x-rays incident on the pore ends.

We can develop an expression for the ratio of MCP events to incident photons, a modified “quantum efficiency” denoted  $R$ , in the presence of a TPC. Existing measurements of MCP QE inherently do not resolve any possible effects of the pore ends, providing for some x-ray energy a QE  $Q_x$  that includes whatever complex combination of effects determines whether a given photoelectron is multiplied by the MCP. For a standard bare nichrome-coated MCP ( $L/D=40$ , bias angle= $8^\circ$ , pore diameter= $10 \mu\text{m}$ ) and 1.49 keV x-rays we previously<sup>8</sup> reported  $Q_x \sim 5.6\%$ . If the TPC transmission (87% here including the substrate) is  $T$ , then the contribution of ordinary x-ray detection to the QE is  $TQ_x$ . The TPC produces some number of secondary electrons per photon incident on the Au layer, designated here as  $Y_b$  and showed by Henke *et al.*<sup>9</sup> for our conditions of interest to be approximately 0.03. If these electrons were detected with QE  $Q_e$ , then our first expression for  $R$ ,  $R_{q1}$ , would be

$$R_{q1} = TQ_x + T_p Y_b Q_e, \quad (1)$$

where  $T_p$  is the transmission of the photocathode substrate, 93% here. One might simplistically suppose that all electrons geometrically entering pores are detected so  $Q_e$  is equal to the open area ratio and that there are no other complicating effects, obtaining  $R_{q1} = 6.7\%$ .

Two points are worth making about this result. First,  $R_{q1}$  is not truly a QE because a single x-ray photon absorbed in the TPC often produces more than one secondary electron.<sup>5</sup> The numbers above correspond to the production of one rear-surface secondary electron for every two absorbed x-ray photons. At this level of emission, the most common emission event will be the emission of a single photoelectron. Second, the value obtained would represent a relatively small increase in detector performance, but this reflects our use of  $Y_b$  for a gold photocathode. As  $Y_b$  is one to two orders of magnitude larger for CsI, the potential increase in detector performance is quite large. In this context, the value of the present work is in testing the fundamental behavior of a TPC, and in learning what improvement may be possible with Au, a more rugged and durable photocathode material. For example, for a solid CsI thicknesses of  $h=0.1 \mu\text{m}$  and  $E_x=1.25 \text{ keV}$ , we find from Fig. 4 by Fraser<sup>5</sup> that  $T=0.25$  and  $Y_b=1.66$ , which yields  $R_{q1} \sim 167\%$ , assuming  $Q_x(1.25 \text{ keV}) \sim 5\%$ . The QE in this case, defined as the number of electron-producing events per incident photon, is 20%. One may argue that the same increase in QE can be achieved if the CsI is directly coated into the MCP pores. However, due to the hygroscopic nature of CsI, the lifetime of a CsI coating is in many cases less than the duration of an experiment, and so implementing an independent and basically disposable CsI TPC could prove valuable.

Returning to the effects of the pore ends in the presence of the TPC, they are twofold. First, the modification of the field structure may lead to an increase in the number of photoelectrons produced on the MCP surface that are subsequently detected. This could potentially increase  $R$  by about 50%, contributing up to  $\sim 2.5\%$  in QE. We write the effect of this on  $R$  as  $\Delta_x$ . Second, the modification of the field structure by the TPC may cause the fraction of the secondary electrons from the photocathode that are detected to differ from the first estimate, equal to the open area. We will view this effect as a variation in  $Q_e$ . In the present case, the maximum potential impact of this on  $R$ , if all such electrons were detected, would take  $Q_e$  to 1 and increment  $R$  by  $\sim 0.9\%$ . Together, this gives

$$R = TQ_x + \Delta_x + T_p Y_b Q_e.$$

Adding all these effects to the maximum value of  $R$ , we might expect to find here  $\sim 10\%$ . In the present case, as discussed below, our data indicates that the observed signal is produced predominately by single-secondary-electron events. This implies that  $R$  can sensibly be interpreted as an approximate QE, and we describe the result as a QE measurement below.

There is a trade-off between QE and resolution of the TPC/MCP assembly. The potential difference should be adjusted so that the QE is maximized for the specific MCP geometry, yet at the same time this potential difference must

be tuned such that it turns electrons from the inter-pore space and deposits them near their original creation site. If the field is too large the electrons will return exactly to their creation site and will not be detected. However, if the field is too small the electrons will be deflected many pores away from their creation site, thus decreasing the resolution. The final resolution element size is an important parameter in determining the acceptable electron spreading. For example, if the object plane resolution is  $10\ \mu\text{m}$  and the imaging diagnostic is operating at  $20\times$  magnification, then the resolution element in the image plane would be  $200\ \mu\text{m}$ . In this case, electrons generated in the inter-pore area can wander approximately  $200\ \mu\text{m}$  from their creation site without any significant loss of imaging resolution. Resolution measurements in the present system are discussed below.

### III. EXPERIMENTAL SETUP

Our experimental system, evacuated by a turbomolecular pump backed by a scroll pump, operates at a pressure of  $10^{-7}$  Torr. Mounted to it is a direct-current Manson source, operated for the present study with an aluminum anode that emits photons of  $1.49\ \text{keV}$  ( $\text{Al } K\alpha$ ). The x-ray source has a spot size of approximately  $1\ \text{mm}$ . X-rays propagate down two beamlines at equal angles relative to the normal vector to the anode. One of these is incident onto the detector arrangement of interest and the other is incident onto an absolutely calibrated IRD AXUV-100 photodiode, which measures the x-ray flux and allows us to determine the flux incident onto the detector system under study. The detector system is composed of the TPC (when present) and the MCP, followed by a phosphor-coated fiber-optic faceplate (using a  $P-43$ ,  $\lambda=540\ \text{nm}$  phosphor). The output of the fiber-optic faceplate is lens coupled to an optical charge coupled device camera.

The present work used our system for mounting and testing  $1\ \text{in.}$  diameter MCPs, built with the goal of evaluating a number of options for improvements to MCP performance. The mounting system creates a good vacuum seal at the edges of the fiber-optic faceplate, without obscuring the plate, and keeps the phosphor surface of the faceplate at a very precise distance from the MCP rear surface. The MCP is held without undue stress. Voltage is supplied, via vacuum feedthroughs, to the MCP and the phosphor. In addition, the mounting system can support and provide voltage to a circular component mounted some distance above the front surface of the MCP. In the present work this component was the TPC, mounted  $210\ \mu\text{m}$  above this surface, which is the closest possible distance based on our current camera design. The MCP was nichrome coated and was operated at a potential of  $-900\ \text{V}$ . The phosphor was operated at  $+4000\ \text{V}$ , which has been shown to produce the largest MCP gain while preventing any electrical breakdown between the plates. The potential of the TPC was varied from  $0$  to  $-1800\ \text{V}$ .

The photocathode utilized for this work is composed of  $160\ \text{\AA}$  of Au (99.99% purity) vapor deposited onto a  $1\ \mu\text{m}$  thick polystyrene film, and oriented so the Au surface faced the MCP. The polystyrene film transmits about 93% of the

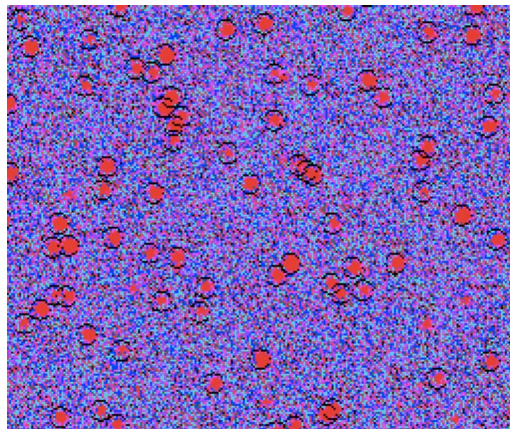


FIG. 2. (Color online) One data image. The dots in the image are events in which a burst of amplified electrons has struck the phosphor and been detected. The circles show those events identified by the star-finding routine called FIND, provided on NASA's Astronomy User's Library.

incident x-rays to the Au layer. The Au layer absorbs 6% of the photons that strike it. Thus, the combined transmission of the polystyrene and the Au was 87%.

### IV. METHOD

To make measurements relevant to QE, we operated the Manson source so as to obtain 0.01 photons per MCP pore for a 10 ms exposure. Under these conditions, an image obtained from the phosphor resembles that of a starry night. Each star can be interpreted as a single photon event, as the probability of a two-photon event is negligible. The observed characteristic spatial full width at half maximum (FWHM) of these events is  $\sim 50\ \mu\text{m}$ . We used a modified star-finding program, discussed previously,<sup>8</sup> to determine the number of such events. Figure 2 shows an example, with the circles showing the location of the events that were identified. Some weak, uncircled dots can be seen in the image. These were below the threshold set to correspond to an event, and would contribute insignificantly to the total signal intensity in a typical imaging application having many events per resolution element. The events are of varying amplitude, as previously discussed.<sup>8</sup> We examined the pulse-height distribution of these events with and without the TPC, finding no significant difference between the two cases.

In order to interpret the observed signal in terms of a QE in the case of the TPC, one must also consider whether multiple observed events might be produced by a single photon absorbed in the TPC. This might occur if two or more secondary electrons were emitted in response to the absorption of a single photon in the TPC, and if these electrons struck the MCP with a separation larger than the  $50\ \mu\text{m}$  FWHM characteristic of single events. We assessed this as follows. The secondary electron distribution is Lambertian so that half of the secondaries are emitted at an angle larger than  $45^\circ$  from the surface normal. Their characteristic energy is  $3\ \text{eV}$ .<sup>9</sup> A  $3\ \text{eV}$  electron emitted at  $45^\circ$  degrees and then crossing  $210\ \mu\text{m}$  while dropping through a potential difference of  $300\ \text{V}$  moves laterally by  $\sim 30\ \mu\text{m}$ . If one considers cases in which two such electrons are emitted, then under most circumstances in our data less than half of such cases would

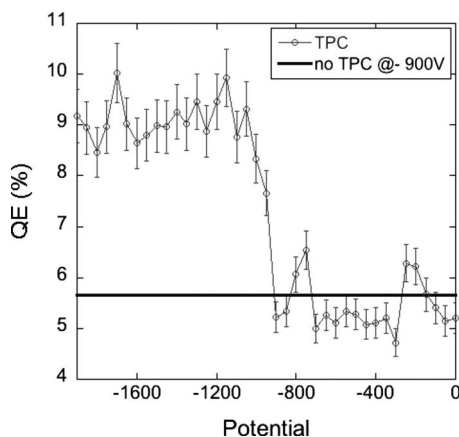


FIG. 3. QE of the system against TPC potential. From photodiode measurements we estimate that  $5432 \pm 270$  photons were incident on the instrument during these measurements. The value of QE for TPC and MCP was determined from the average number of events on five images.

produce well-separated events. This in turn would imply that more than half of such cases would produce events with anomalously high intensity, resulting from the detection of two electrons. We see no evidence in the pulse-height distribution of such an effect, and conclude that the observed events predominately correspond to single detected photons, whether in the MCP or the TPC. Given this conclusion, we evaluate the QE the ratio between the total number of events and the total number of photons incident onto the TPC or MCP per image.

To make measurements of resolution, five images of a razor edge were taken at the each of several PC voltages. All images at a given voltage were first averaged pixel by pixel to reduce noise in the exposed area. The razor edge was then fit to a line and line profiles perpendicular to the edge were taken and averaged, again to reduce noise in the exposed region.<sup>10</sup> Numerical differentiation of the edge response produces the line-spread function, which was fit to a Gaussian peak. From the analytic Gaussian function a Fourier transform yielded the modulation transfer function (MTF). The MTF determined from the fitted Gaussian is in good agreement with a direct Fourier transform of the data (using the fftw function as implemented in MATLAB) and with previous MCP resolution tests.<sup>3,11</sup>

## V. RESULTS

We operated the system with constant Manson-source settings and constant voltages on the MCP and phosphor, varying only the voltage on the TPC. We obtained five images for each voltage and determined the QE as described above. Figure 3 shows the dependence of the QE on the applied photocathode voltage, and shows the results obtained without the TPC as a straight line. The error bars represent the standard deviation of the measurements. At voltages above the voltage of the front surface of the MCP (i.e., between  $-900$  and  $0$  V), the electric field prevents the secondary electrons from the TPC from reaching the MCP. The QE as defined here is typically below the value seen with a bare MCP, as it should be because of the absorption of some x-rays by the photocathode. The expected value in this re-

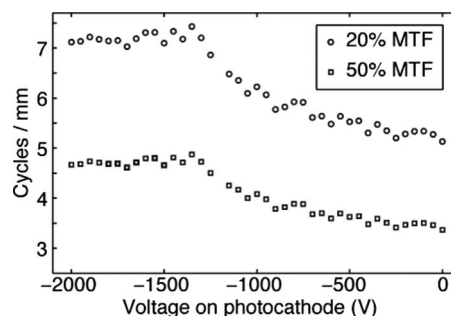


FIG. 4. Dependence of 20% and 50% MTF values on TPC voltage. Above a threshold value of approximately  $-1300$  V the resolution of the imaging system begins decreasing.

gion is 4.9%. As the voltage decreases below  $-900$  V, the QE gradually increases, reaching a value of  $\sim 9\%$  at voltages below  $-1150$  V.

Figure 4 summarizes the results of the MTF measurements. It shows the number of cycles per mm where the MTF reaches 50% and 20% as a function of the photocathode voltage. It is notable that the resolution begins to degrade as the voltage drops below  $-1300$  V, still  $400$  V below the MCP surface voltage. This suggests that the detailed field structure around the pore ends does indeed affect electron transport across the surface. By the time the field reaches  $-1100$  V and the QE is maximized, the resolution in cycles per millimeter has degraded less than 25%. Whether these changes are significant for a given measurement depends on the context. Measurements needing the best possible resolution and having ample signal might best be made with the MCP surface biased to repel electrons away from its surface. Measurements having large resolution elements at the MCP surface, such as single images at high magnification, may benefit more from the increased QE than they suffer from decreased resolution.

## VI. CONCLUSION

We have reported measurements of the signal observed when a gold TPC is suspended above a nichrome-coated microchannel plate. The introduction of the photocathode corresponds to an approximately twofold increase in detected events. This is a larger increase than would be expected from secondary electron production by the photocathode. We have suggested that the increase includes this effect in addition to an increased QE for x-rays that reach the MCP surface, caused by the effect on the photocathode voltage on the electric fields there. To test this conclusion, future work should be undertaken using a reflecting grid to vary the electric field structure without introducing a significant source of additional signal. Resolution studies showed a modest decrease in spatial resolution in the presence of the TPC.

## ACKNOWLEDGMENTS

This work was supported by the Naval Research Laboratory through Grant No. NRL N00173-06-1-G906 and by the Stewardship Sciences Academic Alliances Program via DOE Research Grant No. DE-FG52-04NA00064.

- <sup>1</sup>K. S. Budil, T. S. Perry, P. M. Bell, J. D. Hares, P. L. Miller, T. A. Peyser, R. Wallace, H. Louis, and D. E. Smith, *Rev. Sci. Instrum.* **67**, 485 (1996).
- <sup>2</sup>O. L. Landen, A. Abare, B. A. Hammel, P. M. Bell, and D. K. Bradley, *Proc. SPIE* **2273**, 245 (1994).
- <sup>3</sup>C. J. Pawley and A. V. Deniz, *Rev. Sci. Instrum.* **71**, 1286 (2000).
- <sup>4</sup>G. W. Fraser, *Nucl. Instrum. Methods Phys. Res.* **195**, 523 (1982).
- <sup>5</sup>G. W. Fraser, *Nucl. Instrum. Methods Phys. Res. A* **228**, 532 (1985).
- <sup>6</sup>F. Ze, O. L. Landen, P. M. Bell, R. E. Turner, T. Tutt, S. S. Alvarez, and R. L. Costa, *Rev. Sci. Instrum.* **70**, 659 (1999).
- <sup>7</sup>G. W. Fraser, *Nucl. Instrum. Methods Phys. Res.* **206**, 445 (1983).
- <sup>8</sup>E. C. Harding and R. P. Drake, *Rev. Sci. Instrum.* **77**, 3 (2006).
- <sup>9</sup>B. L. Henke, J. P. Knauer, and K. Premaratne, *J. Appl. Phys.* **52**, 1509 (1981).
- <sup>10</sup>E. Samei, M. J. Flynn, and D. A. Reimann, *Med. Phys.* **25**, 1 (1998).
- <sup>11</sup>M. Frigo and S. G. Johnson, *Proc. IEEE* **93**, 216 (2005).